ARMY RESEARCH LABORATORY

Using the Advanced Research Version of the Weather Research and Forecast Model in Support of ScanEagle Unmanned Aircraft System Test Flights

by Jeffrey E. Passner, Robert E. Dumais, Jr.,
Robert Flanigan, and Stephen Kirby

ARL-TR-4746   **March 2009**

NOTICES

Disclaimers

Army Research Laboratory

White Sands Missile Range, NM 88002-5501

Using the Advanced Research Version of the Weather Research and Forecast Model in Support of ScanEagle Unmanned Aircraft System Test Flights

**Jeffrey E. Passner, Robert E. Dumais, Jr.,
Robert Flanigan, and Stephen Kirby**
Computational Information Sciences Directorate, ARL

REPORT DOCUMENTATION PAGE

Public reporting burden for this collection of information is estimated to average 1 hour per response, including the time for reviewing instructions, searching existing data sources, gathering and maintaining the data needed, and completing and reviewing the collection information. Send comments regarding this burden estimate or any other aspect of this collection of information, including suggestions for reducing the burden, to Department of Defense, Washington Headquarters Services, Directorate for Information Operations and Reports (0704-0188), 1215 Jefferson Davis Highway, Suite 1204, Arlington, VA 22202-4302. Respondents should be aware that notwithstanding any other provision of law, no person shall be subject to any penalty for failing to comply with a collection of information if it does not display a currently valid OMB control number. **PLEASE DO NOT RETURN YOUR FORM TO THE ABOVE ADDRESS.**

1. REPORT DATE *(DD-MM-YYYY)*	2. REPORT TYPE	3. DATES COVERED *(From - To)*
March 2009	Final	Nov 2007–Feb 2009

4. TITLE AND SUBTITLE	5a. CONTRACT NUMBER
Using the Advanced Research Version of the Weather Research and Forecast model in support of ScanEagle Unmanned Aircraft System test flights	
	5b. GRANT NUMBER
	5c. PROGRAM ELEMENT NUMBER

6. AUTHOR(S)	5d. PROJECT NUMBER
Jeffrey E. Passner, Robert E. Dumais, Jr., Robert Flanigan, and Stephen Kirby	
	5e. TASK NUMBER
	5f. WORK UNIT NUMBER

7. PERFORMING ORGANIZATION NAME(S) AND ADDRESS(ES)	8. PERFORMING ORGANIZATION REPORT NUMBER
U.S. Army Research Laboratory Computational Information Sciences Directorate Battlefield Environment Division (ATTN: AMSRD-ARL-CI-EM) White Sands Missile Range, NM 88002-5501	ARL-TR-4746

9. SPONSORING/MONITORING AGENCY NAME(S) AND ADDRESS(ES)	10. SPONSOR/MONITOR'S ACRONYM(S)
U.S. Army Research Laboratory 2800 Powder Mill Road Adelphi, MD 20783-1145	
	11. SPONSOR/MONITOR'S REPORT NUMBER(S)

12. DISTRIBUTION/AVAILABILITY STATEMENT

Approved for public release; distribution unlimited.

13. SUPPLEMENTARY NOTES

14. ABSTRACT

The U.S. Army Cold Regions Research and Engineering Laboratory (CRREL) supported unmanned aircraft flights in a specified airspace domain at Yuma Proving Ground (YPG) in November and December 2007. The Battlefield Environment Division of the Computational and Information Sciences Directorate (CISD), Army Research Laboratory (ARL), was asked to provide real-time meteorological modeling support and weather products such as low-level wind and turbulence forecasts at YPG to help determine areas and times of adverse flying conditions. For each flying period one ARL meteorologist was sent to YPG to provide on-site support and interpretation of the model forecast output and products. The on-site ARL meteorologist was primarily responsible for insuring receipt and proper interpretation of the products for use by flight. This report describes the modeling efforts by ARL and the output of the Advanced Research version of the Weather Research and Forecasting model (WRF-ARW).

15. SUBJECT TERMS

Mesoscale, WRF, evaluation, turbulence

16. SECURITY CLASSIFICATION OF:			17. LIMITATION OF ABSTRACT	18. NUMBER OF PAGES	19a. NAME OF RESPONSIBLE PERSON
a. REPORT	**b. ABSTRACT**	**c. THIS PAGE**	UU	42	Jeffrey E. Passner
Unclassified	Unclassified	Unclassified			19b. TELEPHONE NUMBER *(Include area code)* (575) 678-3193

ii

Contents

List of Figures

List of Tables

Acknowledgments

Summary

The U.S. Army Cold Regions Research and Engineering Laboratory (CRREL) unmanned aircraft flights in a specified airspace domain at the Yuma Proving Ground (YPG), AZ in November and December 2007. The Battlefield Environment Division of the Computational and Information Sciences Directorate (CISD), at the U.S. Army Research Laboratory (ARL), was asked to provide real-time meteorological modeling support and associated weather products such as local low-level wind and turbulence forecasts to assist in determining areas and times of adverse flying conditions. ARL supported the two flying periods and used high-performance computing resources located at Aberdeen Proving Ground, MD to run the Advanced Research version of the Weather Research and Forecasting model (WRF-ARW). During each exercise, one on-site ARL meteorologist was available to provide support and interpretation of the model forecast output and products. These model runs and their output provided a better understanding of the vertical profiles of winds, temperature, and turbulence for the local flying environment at YPG each day during the test.

INTENTIONALLY LEFT BLANK.

1. Introduction

The Battlefield Environment Division of the Computational and Information Sciences Directorate (CISD) at the U.S. Army Research Laboratory (ARL) has an interest in high spatial and temporal resolution weather output with an emphasis on fine-resolution, short-range forecasts in complex terrain. Thus, when the U.S. Army Cold Regions Research and Engineering Laboratory (CRREL) supported unmanned aircraft flights at Yuma Proving Ground (YPG), AZ in November and December 2007 it incorporated the modeling skills of ARL. These modeling skills provided real-time meteorological support and associated weather products such as local low-level wind and turbulence forecasts at YPG to help determine areas and times of adverse flying conditions. The Advanced Research version of the Weather Research and Forecasting model (WRF-ARW) was run each day of the test with a double-nested configuration centered near the test site location. The outer nest of 3-km grid spacing was configured with a horizontal dimensionality of 171×171, resulting in an areal domain of 510 by 510 km. The inner nest of 1-km grid spacing applied a horizontal dimensionality of 73×73, resulting in an areal domain of 72 by 72 km. The 24-h forecast period commenced at 0000 universal time coordinates (UTC) using the preceding 1200 UTC North American Mesoscale model (NAM) output as input on the evening prior to a planned flight launch, which indicates that at flight time the mesoscale forecast fields should have been clear of any initial noise that may have been introduced through the cold start from the NAM. Additionally, allowing the model to integrate forward a full 24 h, provided a capability to forecast through a diurnal cycle. Each test day provided a variety of weather conditions and the on-site ARL meteorologist furnished a pre-flight briefing and displayed model output of the local boundary-layer wind fields and turbulence forecasts that were used for flight decisions. During the ScanEagle tests at YPG, it was discovered on the 1-km grid that the forecasted intensity of turbulence was excessive in many cases, thus providing a very useful result from the experiment. Additionally, ARL investigated how the local WRF-ARW could be impacted through the assimilation of the local YPG observations (*1*).

2. The Field Experiment

The field exercises, held at YPG during the fall of 2007, focused on testing sensors and communications aboard the ScanEagle Unmanned Aerial System (UAS), which was developed by Boeing and Insitu. Figure 1 shows the Scan Eagle. The dry climate and complex terrain at YPG (located 42 km north of Yuma, AZ), is very similar to many desert locations in the world. The region generally has clear skies and light winds and is ideal for testing aircraft (*2*).

Figure 1. A U.S. Marine holds a ScanEagle.

The ScanEagle carries an inertially stabilized electro-optical and/or infrared camera on a light-weight stabilized turret system integrated with communications range over 100 km and flight endurance of over 20 h. The ScanEagle has a 3-m wingspan and can fly up to 139 km/h. Additionally, the ScanEagle needs no airfield for deployment. Instead, it is launched using a pneumatic launcher designed as part of a university engineering design project, now patented by Insitu as the "SuperWedge" launcher (figure 2). It is recovered using the "SkyHook" retrieval system, which uses a hook on the end of the wingtip to catch a rope hanging from a 15 m pole as shown in figure 3. This is made possible by a high-quality differential Global Positioning System unit mounted on the top of the pole and UAS. The rope is attached to a shock cord to reduce stress on the airframe imposed by the abrupt stop.

Figure 2. A ScanEagle in its catapult launcher.
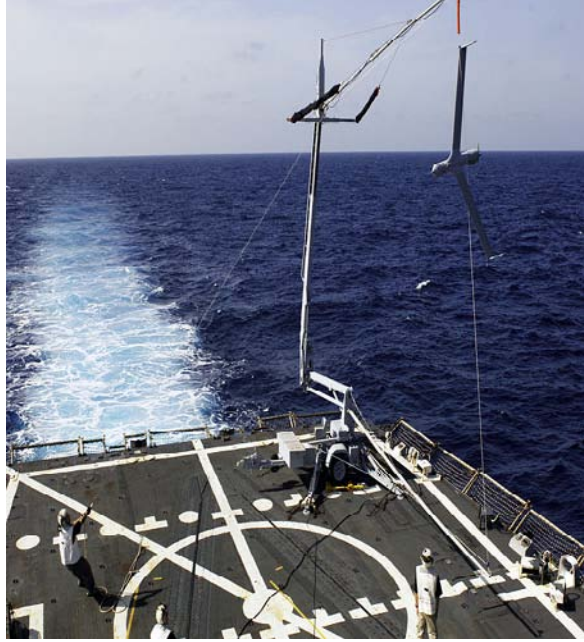
Figure 3. A ScanEagle is recovered at sea.

During the YPG exercises, the ScanEagle flew and conducted tests in both the morning and afternoon hours. The missions ranged from two to five hours in duration and are shown in table 1. The test requirements called for the ScanEagle to fly at approximately 60 m above ground level (AGL); however, as the testing progressed, it flew at even lower levels: 30 and 15 m AGL. As a result, pre-flight forecasts, provided by the ARL on-site meteorologist, emphasized the near-surface weather conditions.

Table 1. ScanEagle flight periods during the two testing periods.

Date	Start time (UTC)	End Time (UTC)
28 Nov. 2007	1600	1900
29 Nov. 2007	1700	2200
30 Nov. 2007	1400	1900
18 Dec. 2007	1500	1900
19 Dec. 2007	2000	2200
20 Dec. 2007	1400	1900
21 Dec. 2007	1400	1900

3. The WRF

The WRF-ARW (hereafter referred to as WRF) model is a next-generation mesoscale weather prediction system designed to serve both operational forecasting and atmospheric research needs. It features multiple dynamical cores, and a software architecture allowing for computational parallelism and system extensibility. The WRF is suitable for a broad spectrum of applications across scales ranging from a few meters to thousands of kilometers (*3*).

3.1 Model Configuration for ARL Study

The WRF runs for this model study were completed using WRF version 2.1.2. To resolve the local terrain features, a double-nested configuration was adopted for the model. The nests were centered near the test site location, at 33.37° N and 114.26° W, as shown in figure 4. The outer nest, displayed to the left with 3 km grid spacing, was configured with a horizontal dimensionality of 171×171, resulting in an areal domain of 510 by 510 km. The inner nest, shown to the right in figure 4 with1-km grid spacing, applied a horizontal dimensionality of 73x73, resulting in an areal domain of 72 by 72 km. The sizes of the two nests were determined so that the outer domain of 3- km resolution was at a ratio of less than 10:1 to the initial and lateral boundary conditions of 32 km. Additionally, the size of the 3-km outer nest needed to be large enough to lessen the effects of the NAM lateral boundary conditions within the center of the inner 1 km grid spacing. Finally, the domain size needed to be small enough for computational considerations and also needed to maintain a 3:1 ratio, if possible, to help eliminate model errors.
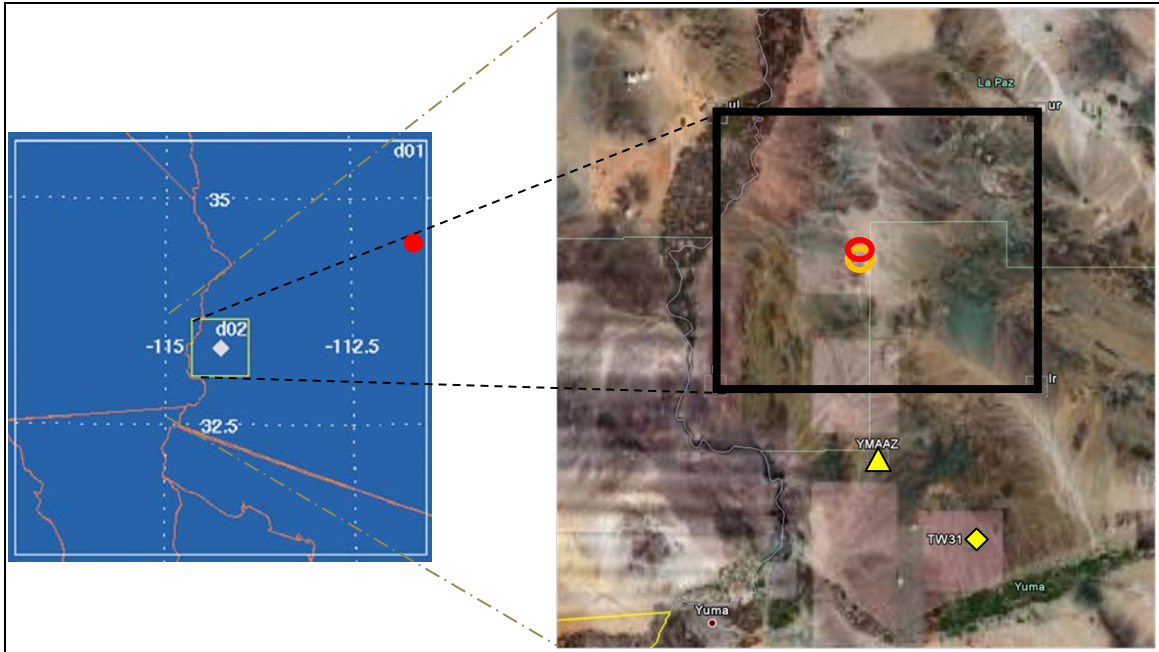
Figure 4. WRF modeling domains with the 3 km (d01) and 1 km (d02) double nesting configuration on the left.

Note: The area surrounding the d02 inner nest is shown on the right, along with the location of the YMAAZ wind profiler (yellow triangle), the TW31 radiosonde site (yellow diamond), the surface met tower site 1 (red oval), and the surface met tower site 3 (orange oval).

The terrain of the test area was a main focus in the model study, since the outer grid contained a variety of desert terrain features with the expected feedback to the local winds. The local terrain is shown in the shaded contour plots displayed for the outer nest in figure 5 and inner nest in figure 6.
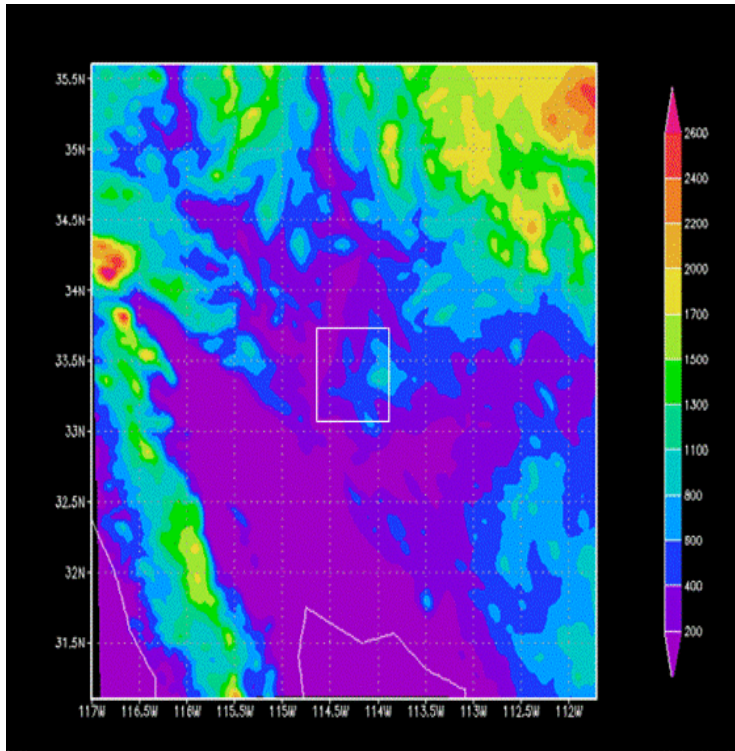
Figure 5. Shaded terrain contours (m) for the 3-km outer WRF nest.
The 1-km grid is shown by the white box.
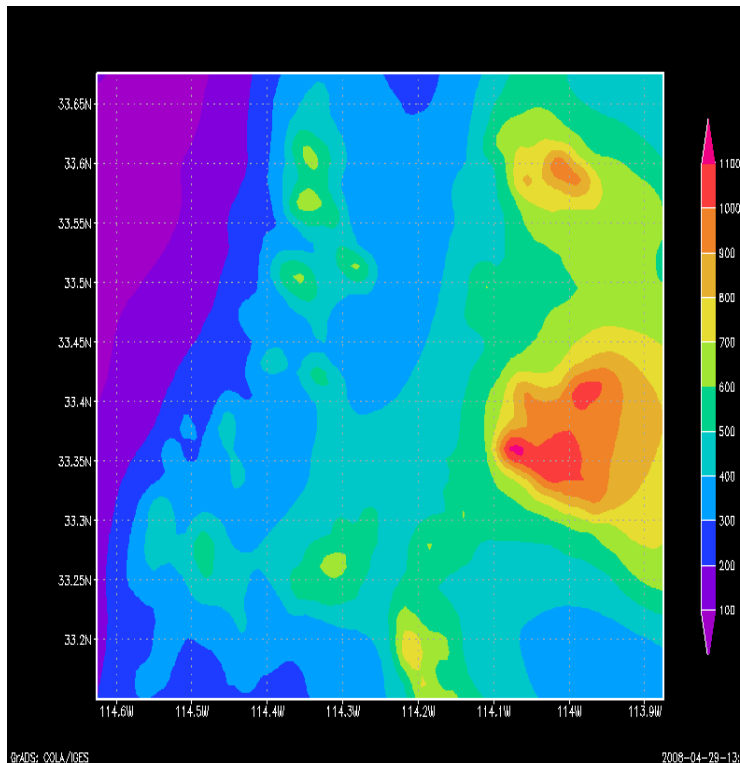
Figure 6. Shaded terrain contours (m) for the 1-km inner WRF nest.

The 24-h forecast period commenced at 0000 UTC, typically the night before a ScanEagle test, using the preceding 1200 UTC NAM for initial conditions. The NAM was developed by the National Center of Environmental Prediction (NCEP) and the dynamic core used is the Non-Hydrostatic model of the Weather Research and Forecasting model (WRF-NMM). Allowing the WRF model to integrate forward a full 24-h provided a capability to forecast through a diurnal cycle. A summary of the WRF-ARW model physics used by ARL follows:

- Lin Microphysics

- No cumulus parmeterization scheme

- W-damping turned on

- 3:1 grid space (km) to time step ratio

- Dudhia short-wave radiation

- Rapid Radiative Transfer Model (RRTM) long-wave radiation

- Noah Land Surface Model

- Mellor-Yamada-Janjic scheme for planetary boundary layer

- Four soil layers

3.2 Turbulence Forecasts

Forecasting clear air turbulence (CAT) is a complicated problem because of the small timescale and resolution at which turbulence is often observed. Theoretical studies and empirical evidence have associated CAT with Kelvin-Helmholtz instabilities. Miles and Howard (*4*) indicate that the development of such instabilities require the existence of a critical Richardson number (RI) <=0.25. Stull (*5*) notes that the RI is a simplified term or approximation of the turbulent kinetic energy equation where the RI is expressed as a ratio of the buoyancy resistance to energy available from the vertical shear.

The equation for the RI is expressed as:

$$RI = \frac{\frac{g}{\theta} * (\frac{\partial \theta}{\partial Z})}{(\frac{\partial V}{\partial Z})^2} \qquad (1)$$

where g is the gravitational acceleration, $\frac{\partial \theta}{\partial Z}$ is the change of potential temperature with height, and ∂V is the vector wind shear occurring over the vertical distance ∂Z.

Numerous scientists have attempted to use both theoretical and observational data to formulate techniques to forecast CAT. Boyle, (*6*) of The U.S. Navy Fleet Numerical Meteorological and

Oceanography Center (FNMOC), used the Panofsky index (PI) to forecast low-level turbulence, where the low level is considered to be below 4000 ft AGL. The formula for this index is:

$$PI = (windspeed)^2 * (1.0 - RI/RI_{crit}) \qquad (2)$$

where RI is the Richardson number and RI_{crit} is a critical Richardson number empirically found to be 10.0 for the FNMOC data. The higher the Panofsky index the greater the intensity of turbulence at low levels.

Ellrod and Knapp (*7*) listed environments where significant CAT was found to be prevalent. Their study associated vertical wind shear (VWS), deformation (DEF), and convergence (CVG) into a single index which is called the Turbulence Index (TI) is expressed as:

$$TI = VWS * [DEF + CVG] \qquad (3)$$

The deformation term is a combination of stretching deformation and shearing deformation.

Originally, of all the methods used to forecast turbulence using a single sounding, the RI seemed to make the most sense physically, since it included the influence of both the temperature and shear in the atmosphere. Based on McCann's work (*8*), the RI also displayed the most skill of several methods tested. However, Passner (*9*) found in his study between 1995 and 1997, that the PI provided more skill than the RI in the lowest 4000 ft AGL using upper-air observation data alone. Knapp et al. (*10*) used Higher Order Turbulence Model for Atmospheric Circulations (HOTMAC) mesoscale model output in their study. HOTMAC was a very course model with only 22 vertical levels and 20-km grid spacing at that time. Knapp noted that the TI was based on the frontogensis equation and the results of his work indicated that DEF+CVG correlated best in the low levels. This implied that horizontal wind flow changes were more vital than vertical motion fields in determining turbulence in the low levels. Passner decided to combine the PI and TI for use in mesoscale model output and used the PI below 4000 ft AGL and the TI above 4000 ft AGL as the way to calculate turbulence from model output.

4. Case Study 1: 28 November 2007

As an example of how the WRF was used on a day without dynamical forcing during the ScanEagle test, the case of 28 November 2007 is shown. The NAM 24-h forecast predicts YPG to lie between an upper low off the Baja California peninsula and a sharp mid-level trough stretching across the Southern Great Basin. The base of the trough contains a strong jet streak over Southern Colorado. Despite weak convergence just south of the Yuma area, the resultant mid-level flow field over YPG is generally light and westerly, although there is a notable low-level northerly wind component predicted for the Colorado River Valley on the 850 hPa chart (not shown). The 24-h forecasted upper-air forecast is displayed in figure 7.
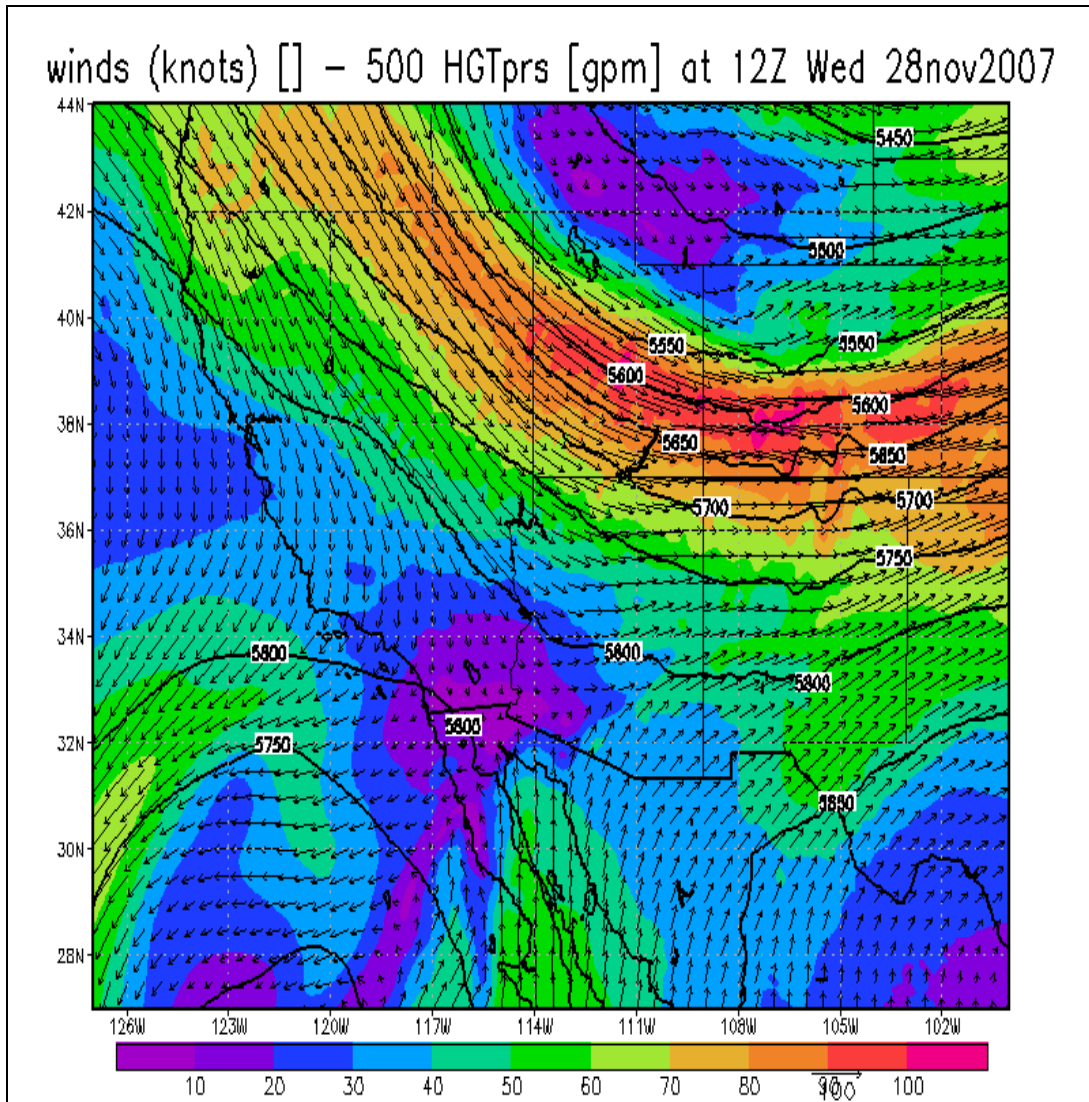
Figure 7. NCEP NAM 24-h 500 hPa forecast over Western United States valid at 1200 UTC 28 Nov. 2007.

The low-level northerly winds are associated with a strong surface high pressure center to the northwest over NV and UT which is enhancing the surface pressure gradient. In addition, there appears to be a cold frontal passage in the early morning hours, with some higher wind gusts forecasted in the afternoon hours.

The NAM-forecasted boundary-layer northerly flow verified based on the observations collected throughout the ScanEagle testing period from 1600 to1900 UTC (not shown). The radiosonde release within YPG, which is displayed in table 2, indicates west to northwest winds. After early morning temperatures fell below 5 °C in isolated areas, afternoon temperatures exceeded 20 °C through much of the YPG region. Given the dry west to northwest surface winds, relative humidity levels remained low throughout the day, and were less than 15% through the early afternoon hours.

Table 2. Radiosonde observations from TW31 site (32.86 N, -114.03 W) during ScanEagle flight test 28 Nov. 2007 at 1634 UTC. Heights are in meters above mean sea level (MSL).

Meters (MSL)	P (hPa)	T (deg C)	RH (%)	Wind Direction (deg)	Wind Speed (m/s)
231	994.6	18.7	16	269	2.1
238	993.8	18.3	17	268	2.3
249	992.5	18.2	17	267	2.5
262	991.0	18.0	18	267	2.6
274	989.6	17.9	18	268	2.8
285	988.3	17.7	18	270	2.8
296	987.0	17.6	19	273	2.8
307	985.7	17.5	19	279	2.8
319	984.4	17.3	19	287	2.6
331	983.0	17.3	19	296	2.5
343	981.7	17.2	19	305	2.5
353	980.5	17.1	19	313	2.5
363	979.3	17.0	19	322	2.6
374	978.0	17.0	19	329	2.7
385	976.8	17.0	19	335	2.9

WRF model results reveal that the 1-km grid forecast did reproduce the northerly post-frontal flow component, although there was some local variability as shown in figure 8. The surface flow modification was more pronounced near the regions of steeper topography, such as the region near the Kofa Mountains (east central part of grid), due to the thermal differences and resultant pressure gradient forces induced by the sloping terrain. This type of diurnal flow behavior is most often observed on days where ambient synoptic forcing or surface pressure gradient is weak. The maximum model afternoon surface temperatures were underforecast by a few degrees (C) near the flight location.
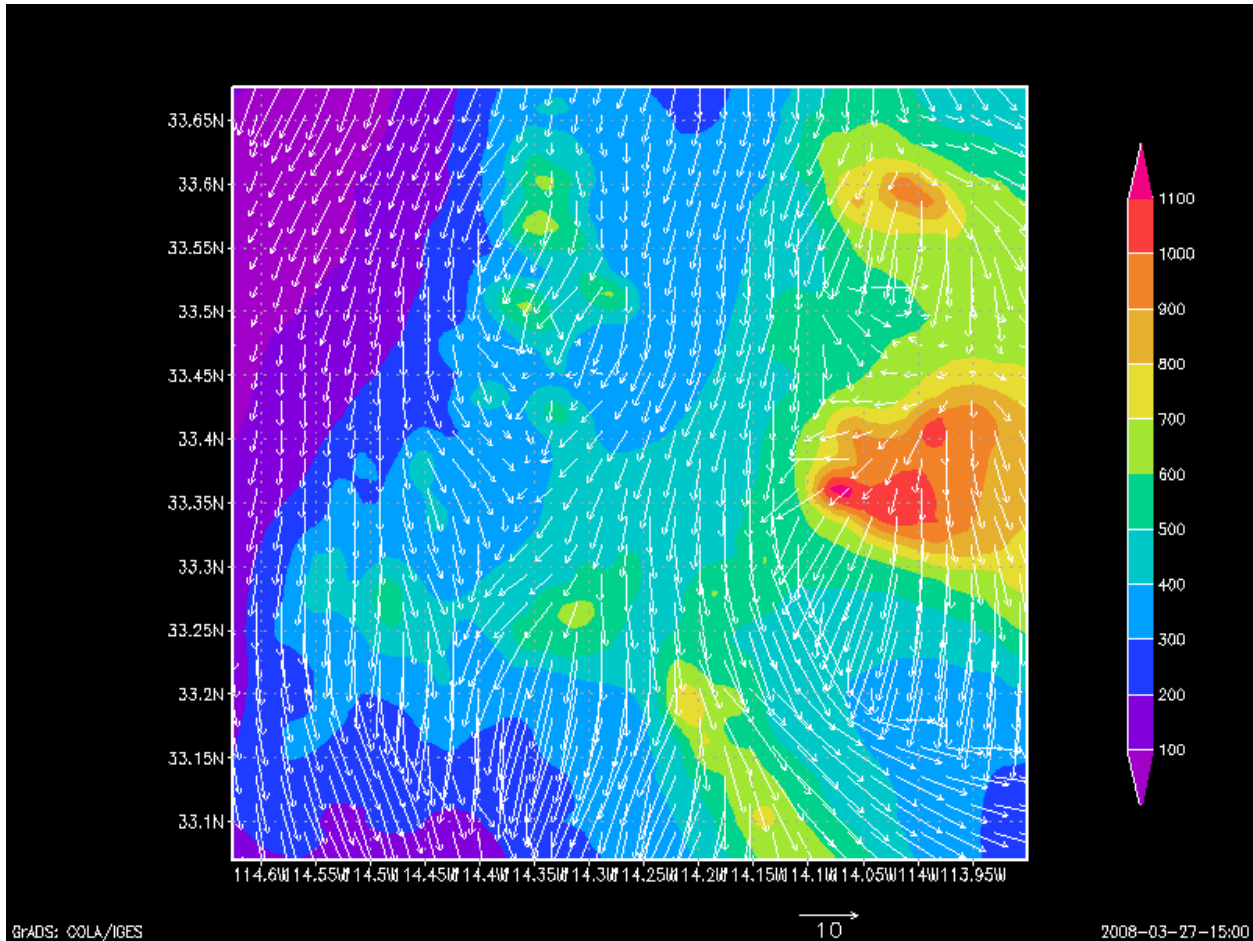
Figure 8. WRF 1-km surface wind fields (m/s) over shaded terrain (m) valid at 1600 UTC 28 Nov. 2007.

5. Case Study 2: 21 December 2007

The operational NAM 24-h 500 hPa forecast chart from 1200 UTC 20 December 2007 is shown in figure 9. The NAM predicted a strong upper-level trough to pass through the region with a 45 m/s jet streak at 500 hPa rounding the base of the trough over Northern Baja California at 1200 UTC 21 December 2007, which was two hours before the start of the ScanEagle flight. A surface frontal passage appears to have occurred between 0600 and 0700 UTC, with the dynamical lift strong enough to produce isolated clouds and light precipitation. Morning winds veered from west to northwest with strong winds gusts observed in the area. Thus, this day provided an interesting case of large-scale synoptic forcing impacting the WRF forecast region, and was an excellent test of how well the model handled the lateral boundary conditions passed to it from the operational NAM. Due to the strong synoptic forcing present throughout the simulation period, local diurnal variability in temperature was minimized.
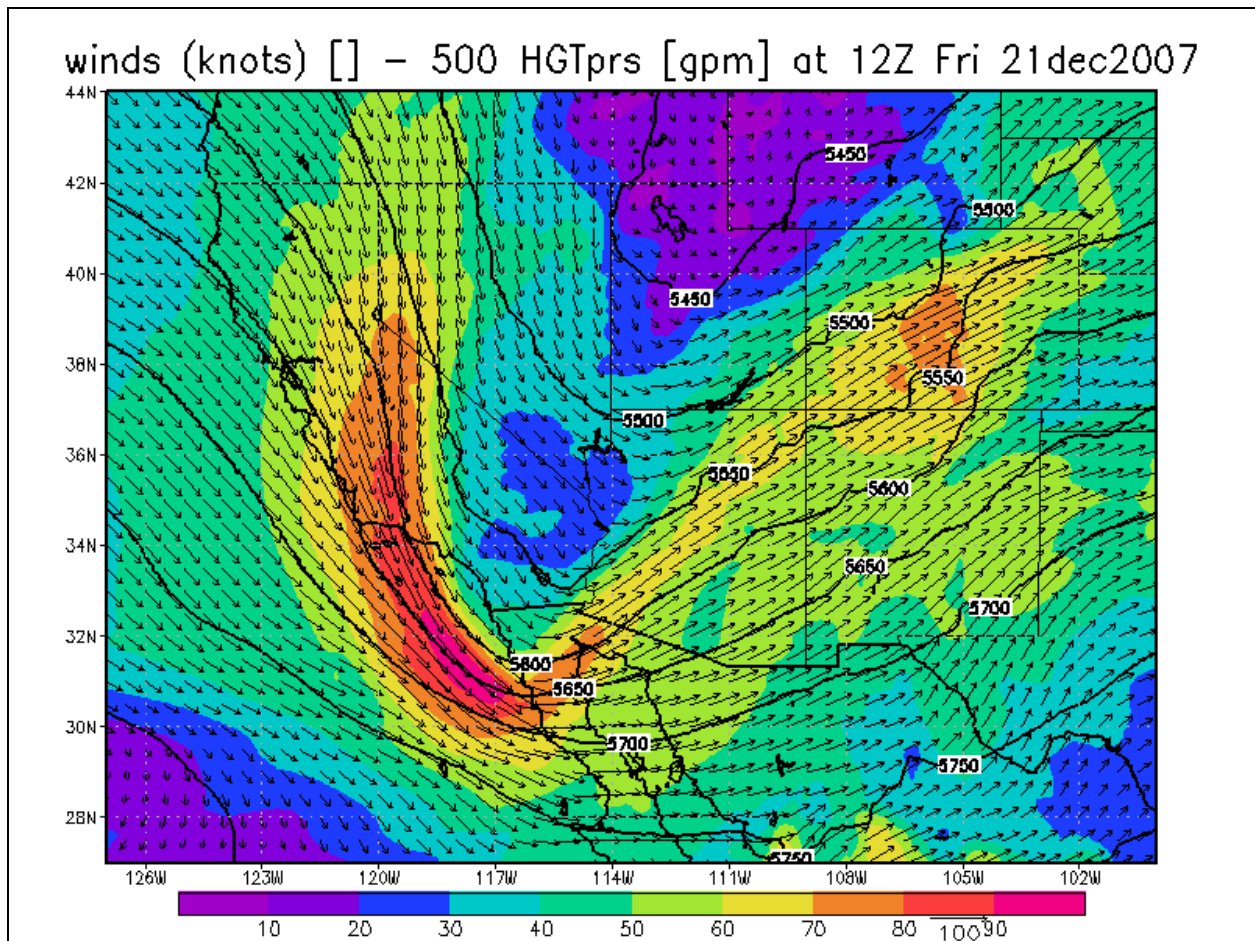
Figure 9. NAM 24-h 500 hPa forecast over southwestern United States valid at 1200 UTC 21 Dec. 2007.

During the ScanEagle flight, from 1400 to 1900 UTC, strong northwest to north winds dominated all levels over the region as shown in figure 10, (reading time from right to left in figure). Temperatures were cool throughout the day, with little variation noted on the grid. Curiously, during the early part of the day there appears to have been a model cold bias of several degrees across much of the region on both the 3-km and 1- km grids as displayed in table 3. By afternoon the model temperature fields were closer to the observed temperature fields.

Subjectively, on this day the model appears to have reproduced the general phases of the meteorological fields quite well, indicating that it had been passed adequate lateral boundary conditions from the NAM as shown in figure 11. The frontal passage was depicted well on both the 3-km and 1-km grids.
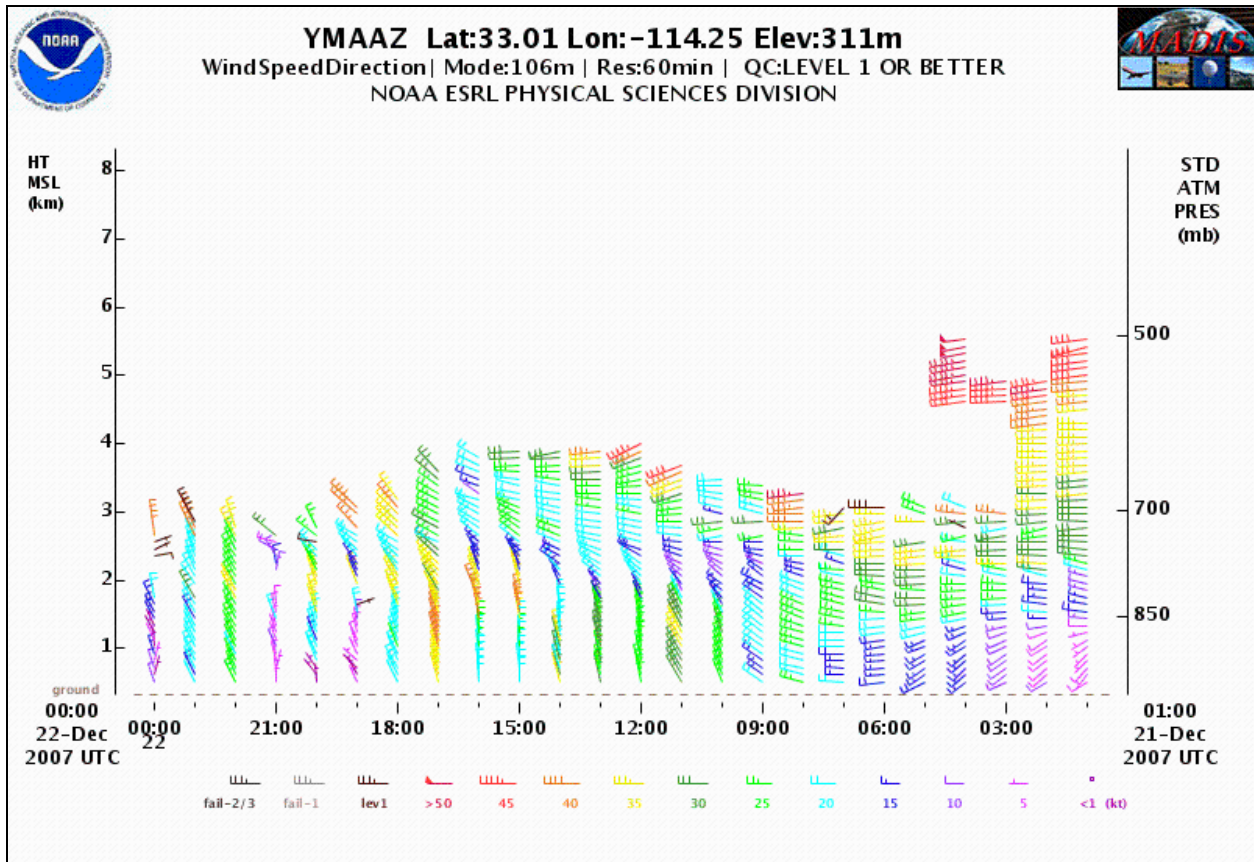
Figure 10. Observations from the wind profiler located at YMAAZ for 21 Dec. 2007.

Note: Source: http://www.madis-fsl.org/cap/profiler.jsp

Table 3. Sites 1 and 3 (blue font) surface weather observations during
the ScanEagle flight test 21 Dec. 2007.

Time (UTC)	Wind speed (m/s)	Wind direction (deg)	T (deg C)
1400	8.3 (9.1)	307.2 (322.3)	9.9 (10.0)
1500	9.0 (8.7)	308.0 (339.2)	9.7 (9.6)
1600	9.0 (7.0)	305.7 (336.8)	10.1 (10.1)
1700	11.2 (7.4)	301.4 (319.0)	10.4 (10.2)
1800	13.5 (6.2)	303.1 (331.9)	10.9 (10.8)
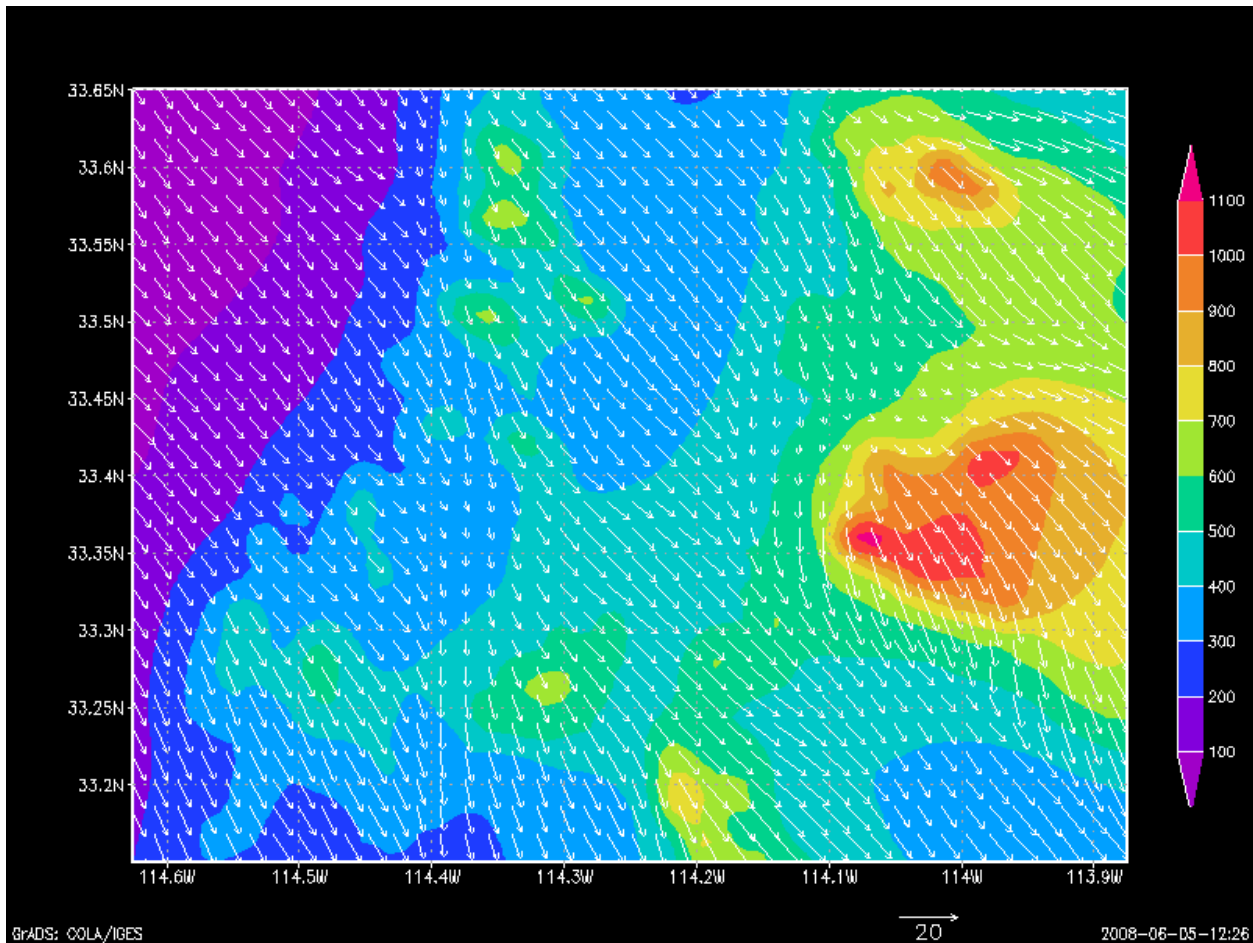
Figure 11. WRF 1-km surface wind fields (m/s) over shaded terrain valid at 1400 UTC 21 Dec. 2007.

6. Post Experiment Efforts and Evaluation

6.1 Data Assimilation Experiment

Once the ScanEagle experiment was concluded, analysis of the modeling efforts and WRF forecasts were commenced in an effort to investigate how short-range forecasts could be impacted through the assimilation using the National Oceanographic and Atmospheric Administration (NOAA) Local Analysis and Prediction System (LAPS). The goal of LAPS is to integrate data from every available meteorological observation system into the model gridded framework.

The test case selected from the ScanEagle experiment was a 24-h simulation period spanning 1500 UTC 28 November 2007 to 1500 UTC 29 November 2007, during which time a detailed temporal coverage of both surface and upper air local weather observations was collected. To

investigate the potential impacts of local data assimilation on the WRF forecasts, the following set of simulations were run:

- initiated with a cold start from NAM (control run with no local data assimilation)

- LAPS-initialized using special YPG three local soundings and surface observations ingested at the initial hour only (data assimilation only applied once, at 1500 UTC 28 November 2007)

- LAPS-initialized using just a single YPG sounding (data assimilation only applied once, at 1500 UTC 28 November 2007)

- LAPS-initialized with all three soundings, but with no data above 700 hPa (data assimilation only applied once, at 1500 UTC 28 November 2007)

- LAPS-initialized with all three soundings, but with no data below 700 hPa (data assimilation only applied once, at 1500 UTC 28 November 2007)

- LAPS-initialized with just special YPG surface observations (data assimilation only applied once, at 1500 UTC 28 November 2007)

The results generated from the 1500 UTC 28 November 2007 runs of the WRF indicate some influence on the model results due to the ingest of the local YPG observations. Although most of the impact seems to have been made upon the model levels in the boundary layer up to the middle levels over the first few hours of the forecasts, some minimal differences can be noted even at 24-h and at higher levels. The model run that ingested only surface observations (not shown) did indicate variation in the moisture forecasts out to 24-h including the upper levels of the model output. While the amount of analysis is very limited in this case, the extent of impact to the short range WRF forecasts due to the local data assimilation, illustrate that differences do occur as shown in figures 12 and figure 13. In figure 12, the 6-h forecast is based on the initialization from the NAM only. In figure 13, the 6-h forecast is based on initialization from NOAA LAPS using three local soundings taken at 1500 UTC and several local surface observations valid at 1500 UTC. The main differences in the local wind direction seem to be near the higher terrain where the northerly winds are enhanced by the east-west ridge axis. There appears to be stronger winds over the ridge top along with more divergence of the surface wind flows because of the terrain.
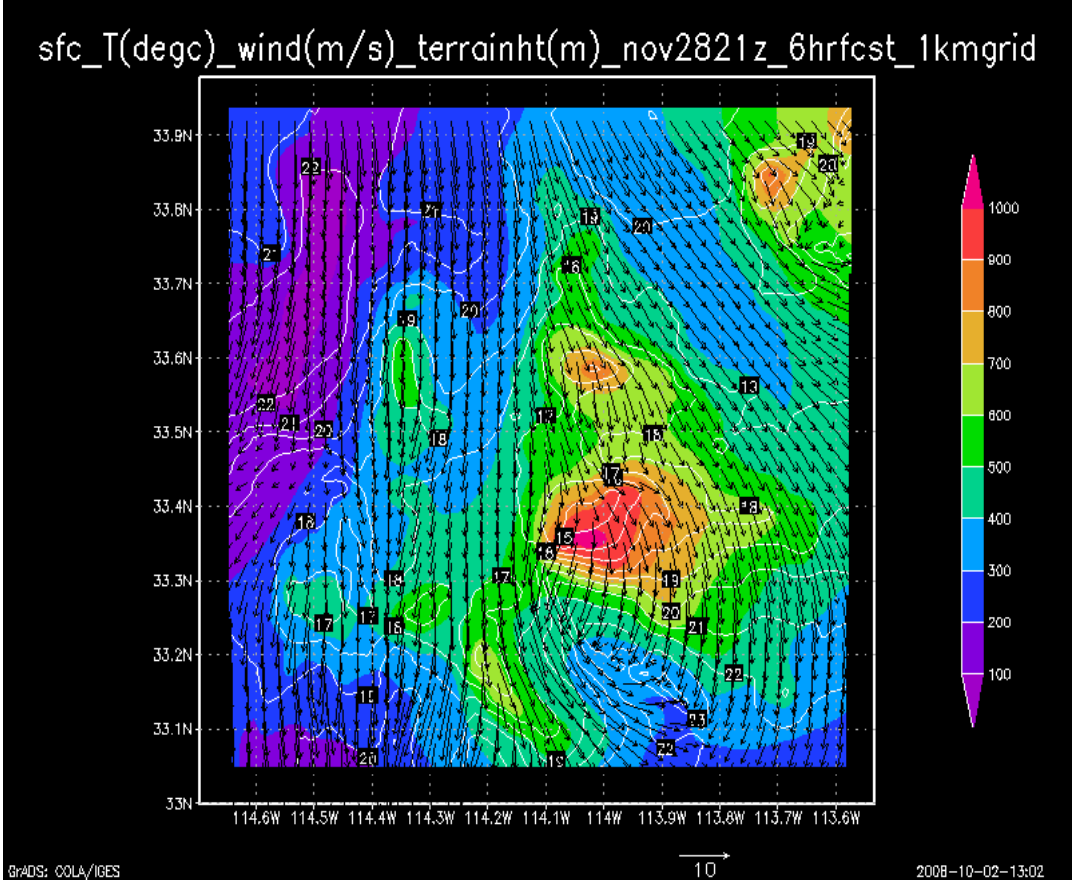
Figure 12. WRF 1-km surface forecast valid 28 Nov. 2007 at 2100 UTC (6-h forecast), based on initialization from the NAM only (no local data assimilation).
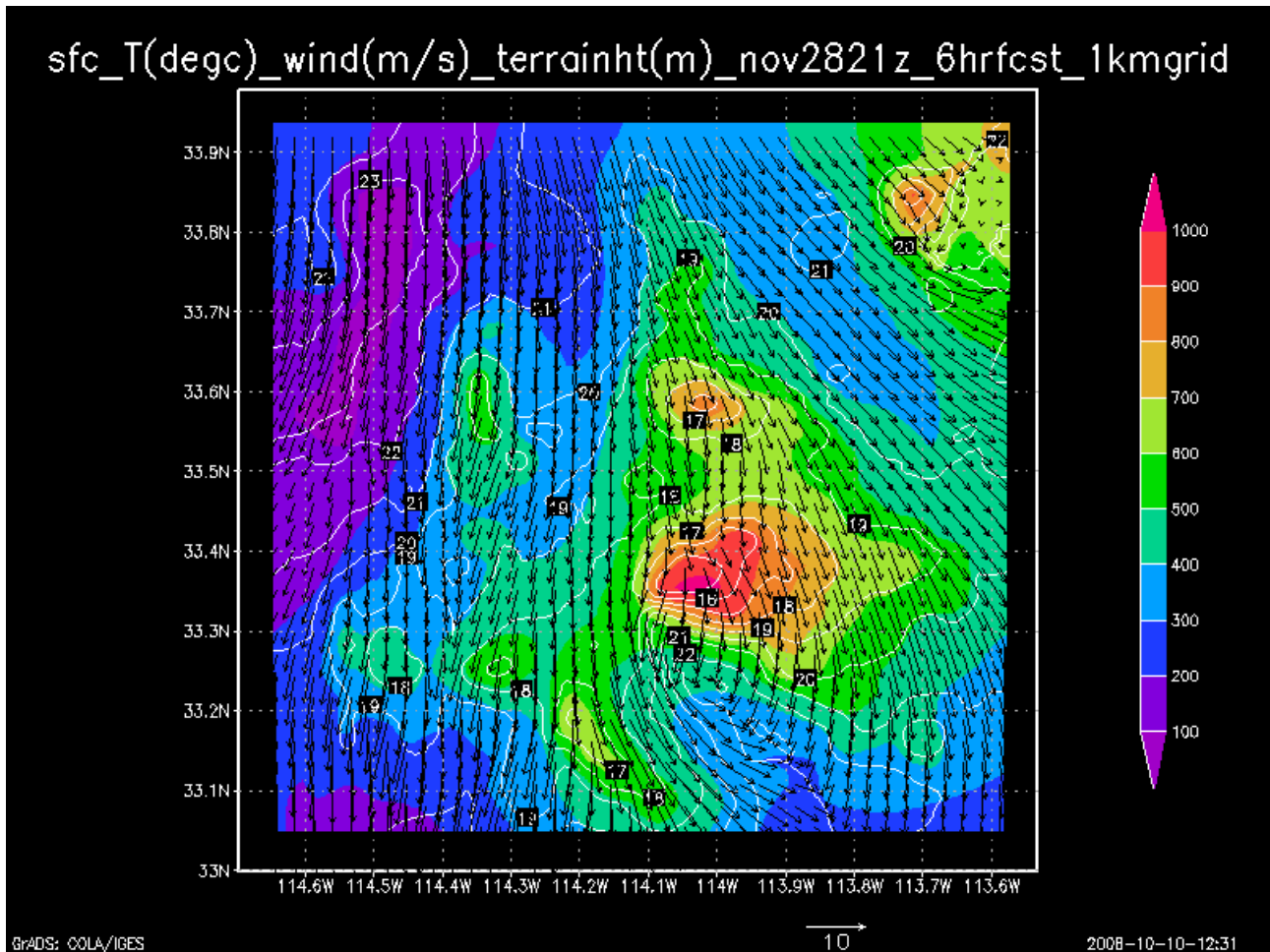
Figure 13. WRF 1-km surface forecast valid 28 Nov. 2007 at 2100 UTC (6-h forecast), based on initialization from NOAA LAPS using three local radiosonde soundings and several local surface observations.

Figure 14 illustrates temperature profiles based on a radiosonde observation compared to the WRF forecasts using the NAM initialization only and using LAPS. The data for this upper-air location are provided in table 4. The difference between model and observation is shown in parenthesis, at each 50 hPa increment from 925 hPa to 400 hPa. Model results were interpolated to pressure levels thus some low-level model smoothing may have occurred. Furthermore, the radiosonde used for this comparison was launched at 1544 UTC 28 November 2007 and is at the same location as the 1440 UTC 28 November 2007 radiosonde launch used in LAPS initialization.

The variations of the data assimilation do not show significant differences in this single case examined, but many more experiments must be completed before any definitive conclusions can be made. It is evident from this case that combining surface and upper-air observations are likely more beneficial than any one data type alone. The dynamics of the model "use" the observations much more consistently when surface and upper air observations are both assimilated. For very fine modeling resolutions, ground state conditions such as soil moisture,

land use, soil temperature, vegetation type, and surface skin temperature probably also are very useful. It is likely that unique combinations of topography, meteorological conditions, and observation density and distribution are critical from case-to-case.
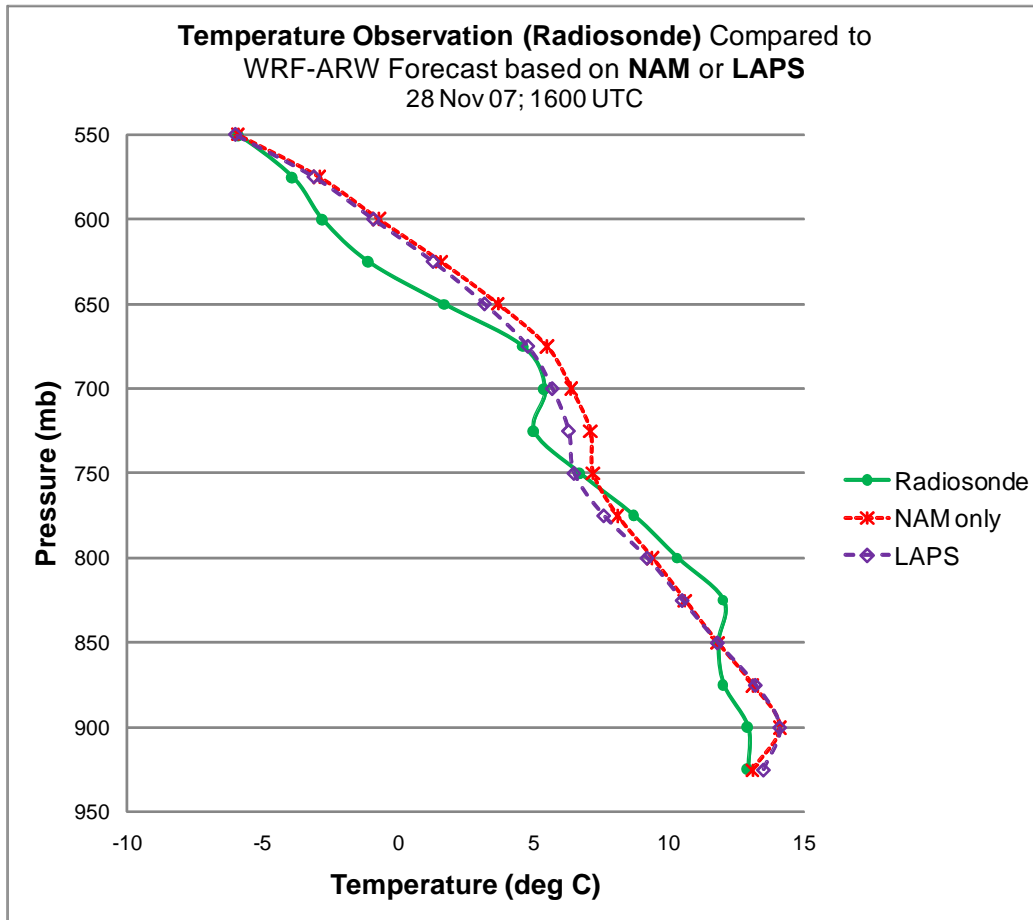

Figure 14. WRF temperature forecasts using NAM initialization only and using LAPS compared to radiosonde observation values.

Table 4. WRF 1-km model temperature at 1600 UTC (1-h forecast) versus 1545 UTC radiosonde observation (33.33 N, -114.33 W) comparing: NAM initialization (cold start) versus LAPS initialization using all three soundings and surface observations.

Pressure Level (hPa)	Radiosonde Observation Temperature (deg C)	NAM Temperature (deg C)	LAPS Temperature (deg C)
925	12.9	13.1 (+0.2)	13.5 (+0.6)
900	12.9	14.1 (+1.2)	14.1 (+1.2)
875	12.0	13.1 (+1.1)	13.2 (+1.2)
850	11.8	11.8 (0.0)	11.8 (0.0)
825	12.0	10.6 (-1.4)	10.5 (-1.5)
800	10.3	9.4 (-1.1)	9.2 (-1.1)
775	8.7	8.1 (-0.6)	7.6 (-1.1)
750	6.7	7.2 (+0.5)	6.5 (-0.2)
725	5.0	7.1 (+2.1)	6.3 (+1.3)
700	5.4	6.4 (+1.0)	5.7 (+0.3)
675	4.6	5.5 (+0.9)	4.8 (+0.2)
650	1.7	3.7 (+2.0)	3.2 (+1.5)
625	-1.1	1.6 (+2.7)	1.3 (+2.4)
600	-2.8	-0.7 (+2.1)	-0.9 (+1.9)
575	-3.9	-2.9 (+1.0)	-3.1 (+0.8)
550	-5.9	-5.9 (0.0)	-6.0 (-0.1)
525	-8.5	-8.9 (-0.4)	-8.9 (-0.4)
500	-11.1	-11.7 (-0.6)	-11.8 (-0.7)
475	-14.4	-14.5 (-0.1)	-14.6 (-0.2)
450	-16.8	-17.3 (-0.5)	-17.4 (-0.6)
425	-20.0	-20.4 (-0.4)	-20.4 (-0.4)
400	-23.3	-23.7 (-0.4)	-23.6 (-0.3)

6.2   Turbulence Evaluation

In this study the unmanned ScanEagle at YPG was typically flown in the lowest levels or boundary layer of the atmosphere between 30 to 90 m AGL, so diagnostic turbulence was calculated using the PI alone. The test was unique since it furnished ARL a chance to investigate turbulence near the surface, which is a layer where pilots rarely fly or have significant time spent in the layer to determine turbulence intensity. Another difference in this test was that the model was run at 1-km grid spacing using 60 model vertical levels. This proved to be problematic due to fine model spacing in the horizontal and vertical. On some test days, turbulence was overforecasted due to the small grid spacing which resulted in excessive values of the RI. This outcome was not surprising given the surface heating and super-adiabatic lapse rates common in the desert even in November and December. Some software changes were implemented during the December part of the study that helped to solve this problem (*11*).

As an example, areas of turbulence were being forecasted over the test domain on 29 November 2007. At noon, the local observations showed a broken layer of cirrus clouds with wind speeds less than 5 m/s with a surface temperature of 21 °C. While boundary-layer turbulence is not well understood, it is uncommon that weather conditions such as those observed would result in moderate or severe turbulence at 1900 UTC, which was being forecasted (figure 15). The red shaded areas are "heavy" or "severe" turbulence, the yellow shaded areas are forecasts of "moderate" turbulence, and the green shaded area is "light" turbulence.
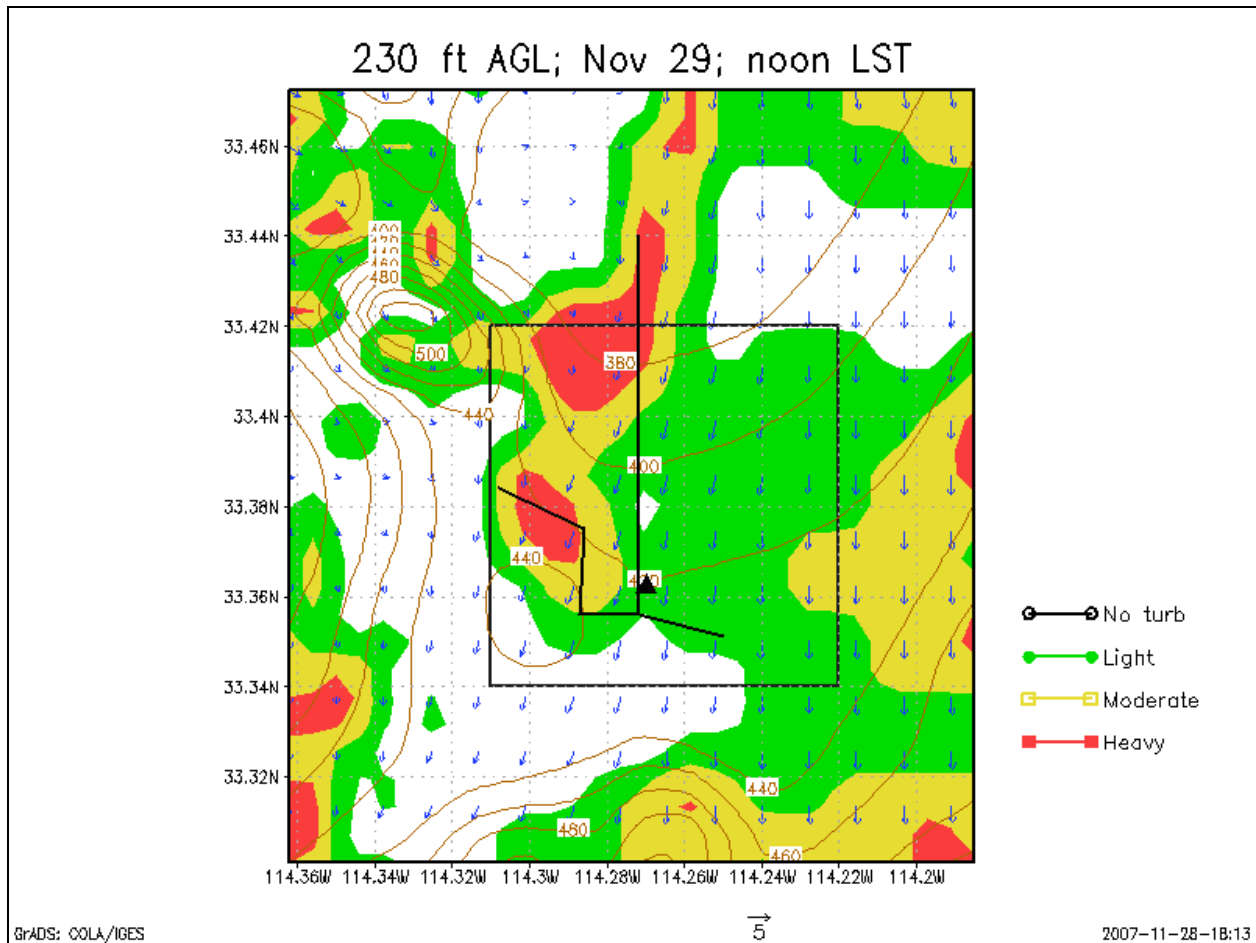

Figure 15. Wind (m/s) and turbulence forecasts at 1500 UTC on 29 Nov. 2007 over YPG. Height contours are displayed in meters MSL.

After adjustments were made in the software to account for the fine resolutions in the horizontal and vertical, the results in figure 16 were much more realistic and indicate no turbulence being forecasted at 70 m AGL.
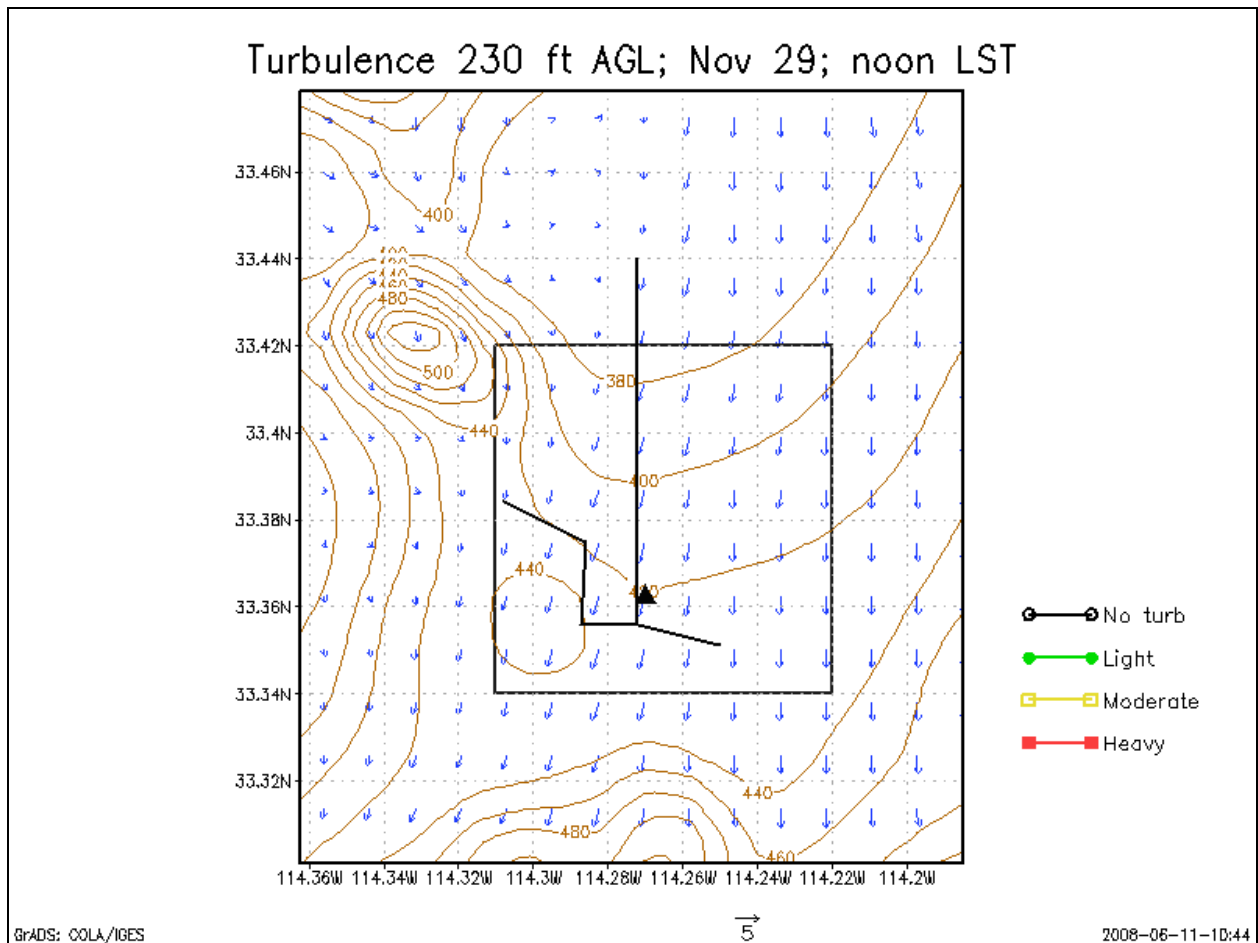
Figure 16. Turbulence forecast for 29 Nov. 2007 at 1900 UTC for 70 m AGL, after software upgrade.

In the next example, the case from 21 December 2007 was investigated. On this day, a cold front passed the Yuma area at about 0700 UTC with the surface winds shifting gradually to the northwest and increasing in intensity during the day. At 1500 UTC, the surface pressure was increasing rapidly, and winds were from 330 degrees at 4 m/s at Yuma. Higher surface winds were noted by observers at the UAS site. The 1-km WRF did an excellent job with the wind direction. Figure 17 shows the plot of forecasted turbulence and winds. However, the turbulence appears to be excessive with severe turbulence (red) forecasted in the southwestern corner of the "box" and moderate turbulence (yellow) over much of the grid. After the software upgrade, much of the severe (or heavy) turbulence was eliminated and most of the grid was covered with moderate turbulence as shown in figure 18.
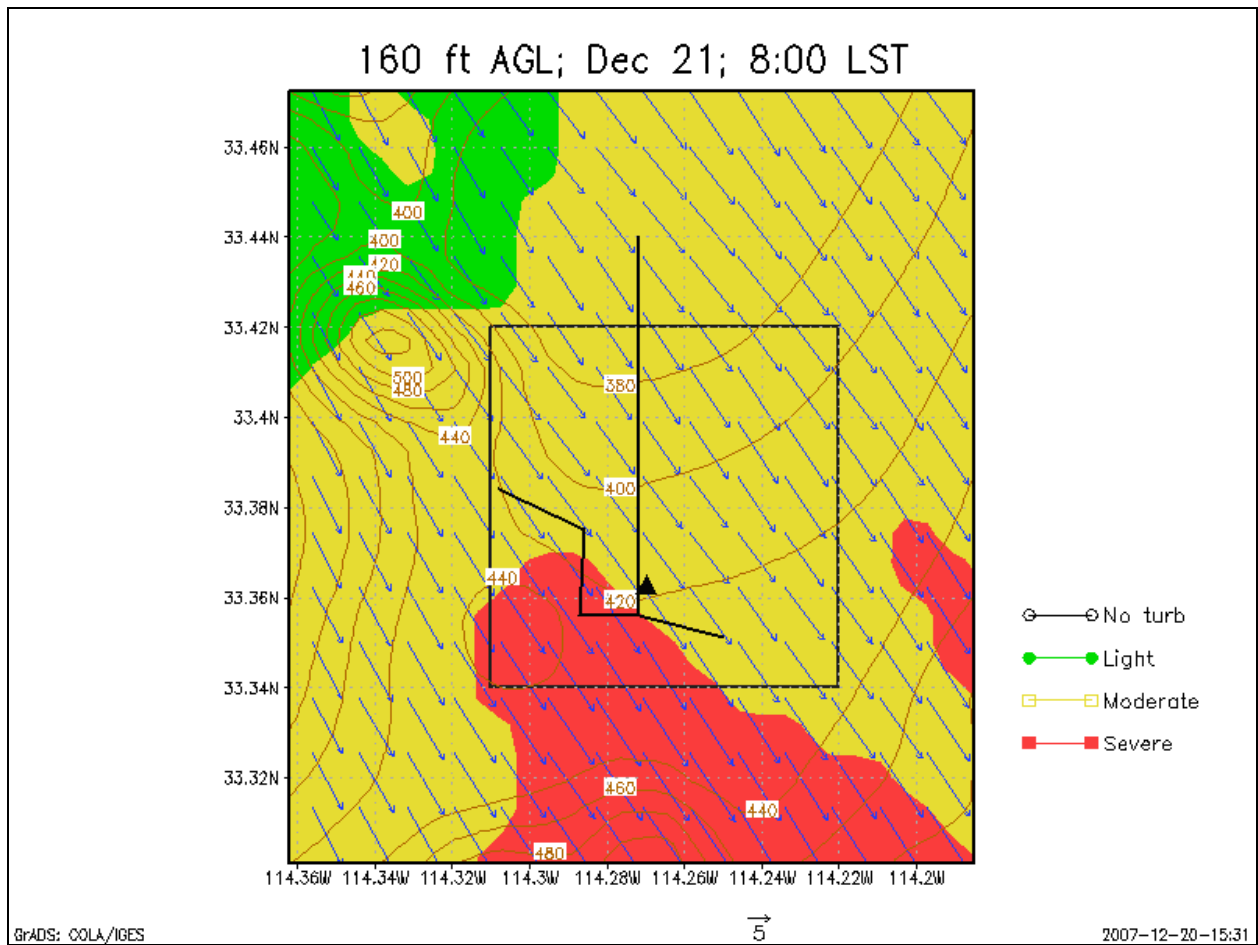
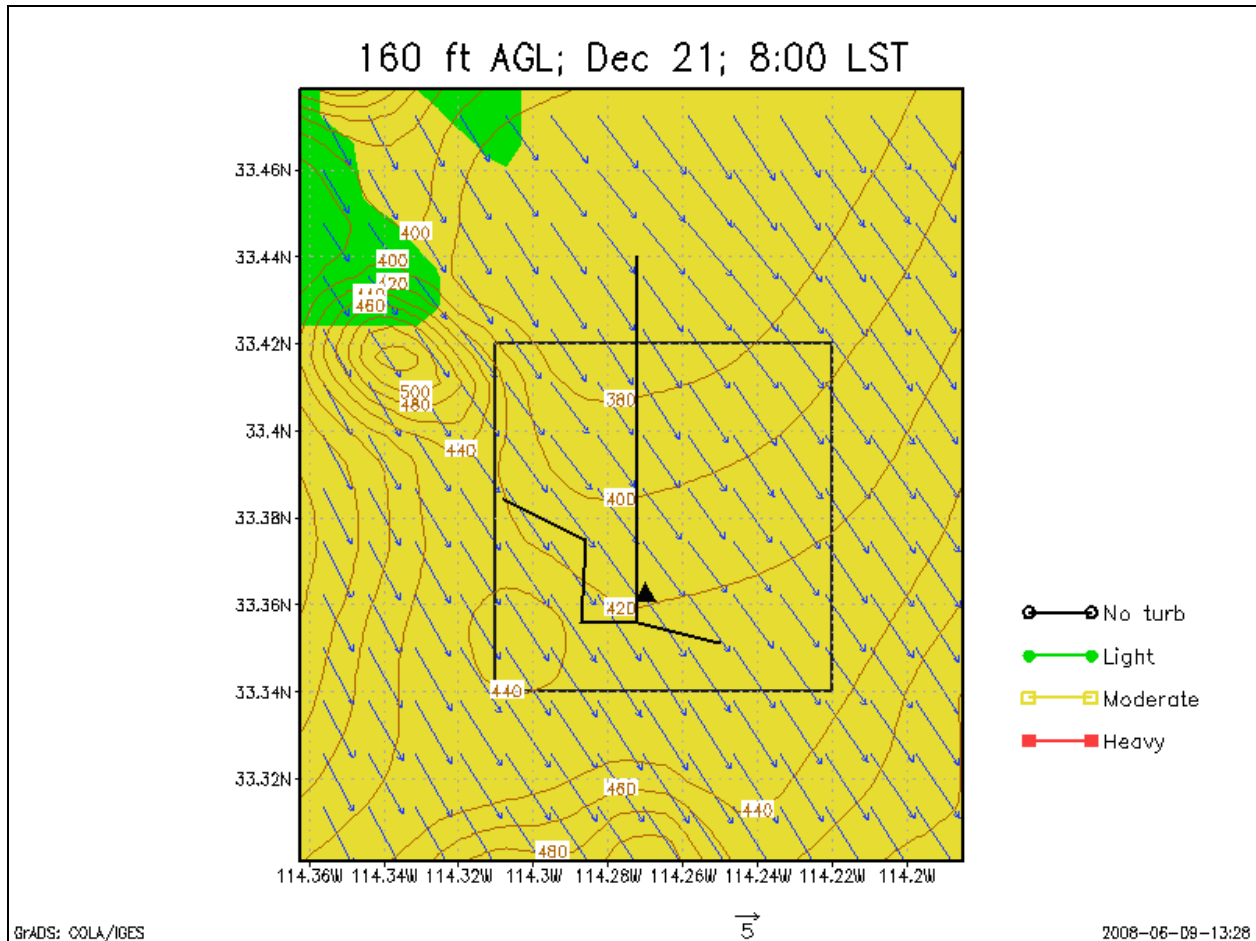Figure 17. Turbulence forecast for 21 Dec. 2007 at 1500 UTC at 48 m AGL.

Figure 18. Turbulence forecast for 21 Dec. 2007 at 1500 UTC at 48 m AGL after software upgrade.

7. Discussion

During the course of the exercise, a variety of weather events provided a challenge for the WRF. Generally, the model performed well, although some local biases were noted. Still, in weak synoptic flow, the model did capture the local flow due to the complex, desert terrain. On the days with stronger weather systems the model also responded to these features and provided guidance that was useful for ScanEagle operations. For example, the model precipitation forecast in figure 19 showed a fairly significant rain event in the area that did verify on 30 November 2007.
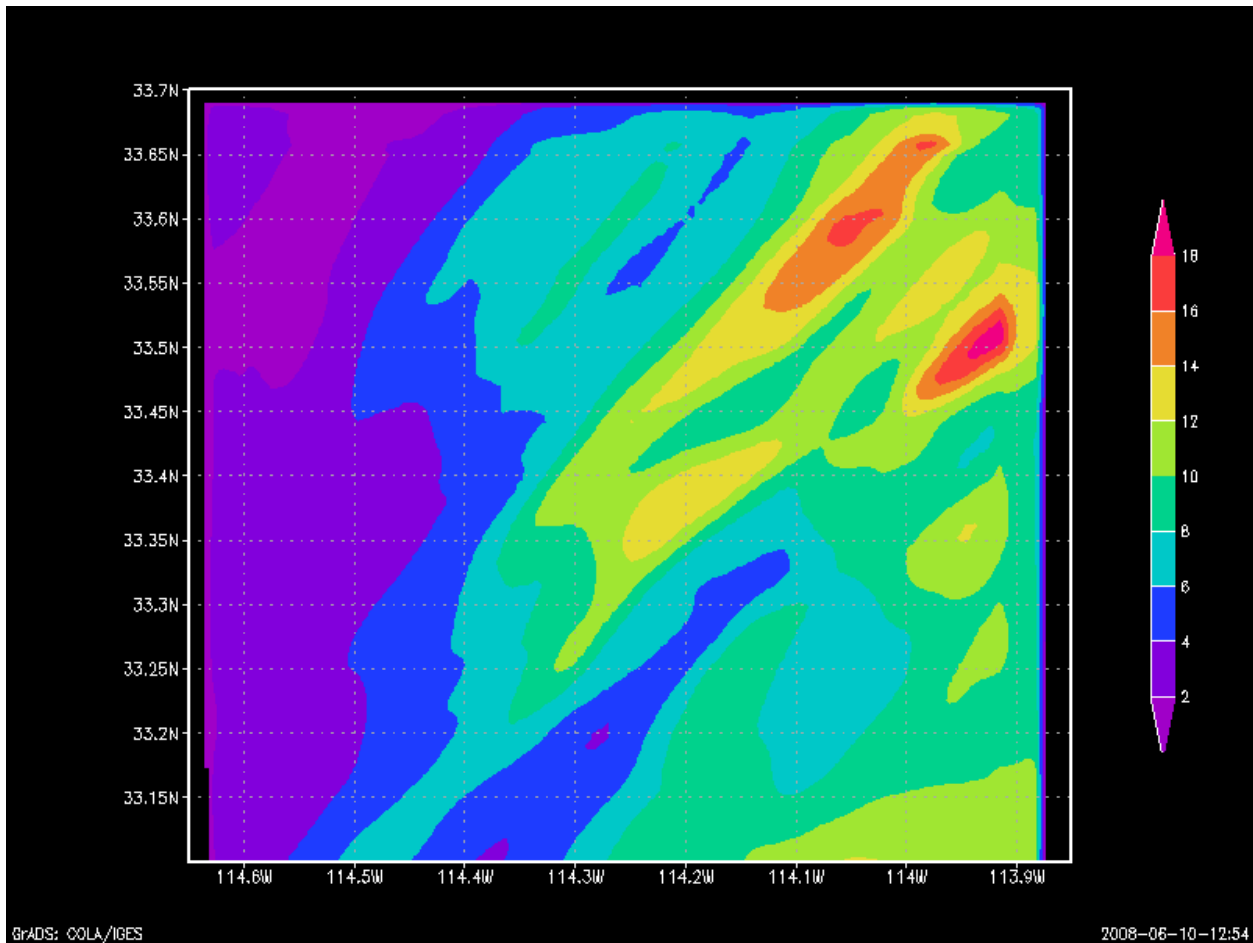
Figure 19. WRF forecast (1-km) of total 24-h accumulated precipitation (mm) valid at 0000 UTC on 1 Dec. 2007.

The dynamical system of 30 November 2007 also provided cloud cover which acted to reduce the incoming short-wave radiation. The model correctly forecasted higher radiation totals in the northwest corner of the grid as shown by the red areas in figure 20. The ScanEagle flight was conducted between 1400 and 1900 UTC so it was completed before precipitation began.

Figure 20. WRF forecast (1-km) of net flux of solar radiation at the surface (W/m^2) valid at 1900 UTC
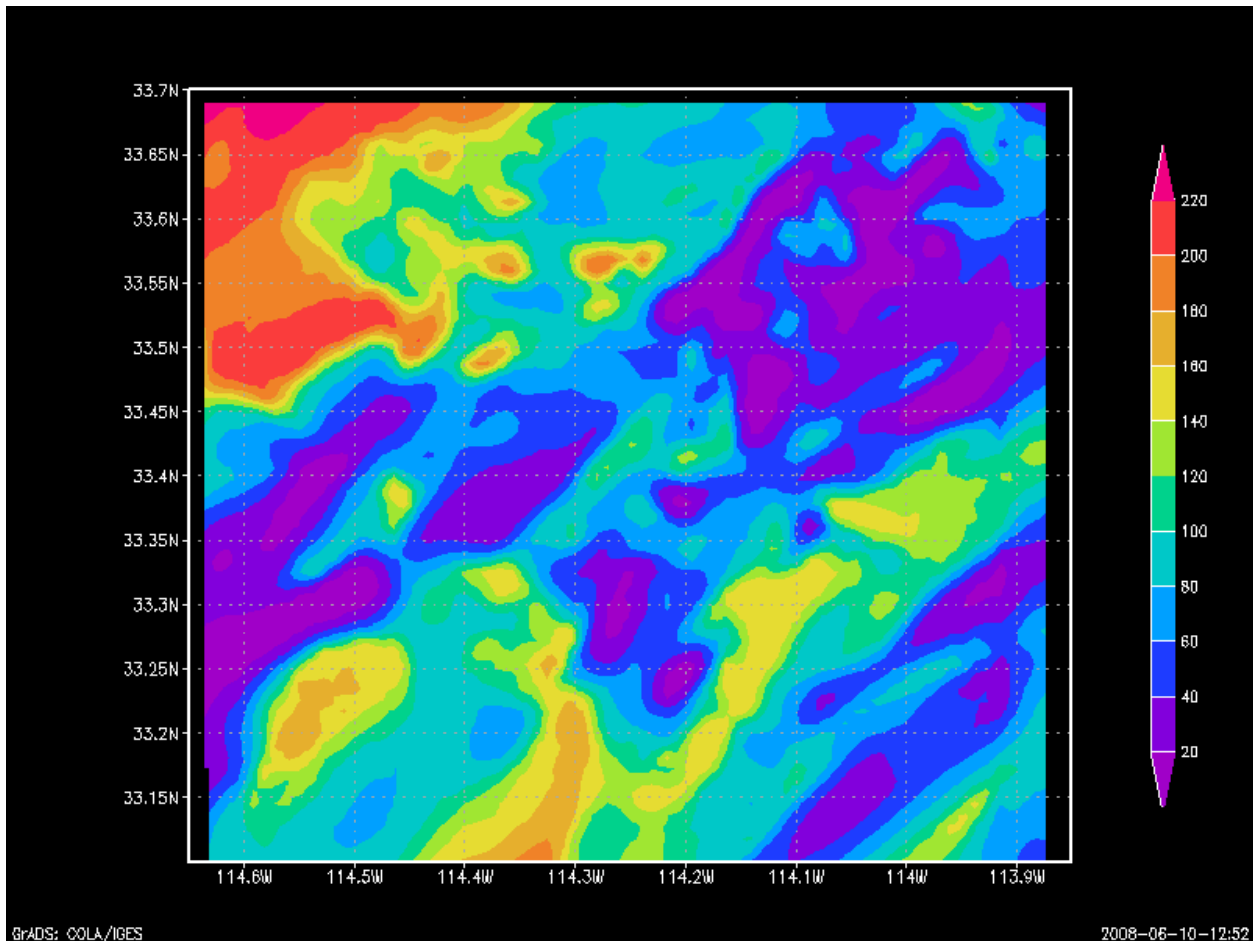30 Nov. 2007.

Temperature forecasts were handled well, except in the northwest corner of the grid where it
appears that the model underforecasted the maximum afternoon temperatures by as much as 4 °C
perhaps because of a premature column moistening over the 1-km grid. Verification of solar
radiation (not shown) indicated more incoming short-wave radiation than the model had
forecasted.

Another model preference noted on many of the morning plots was a bias to miss the areas of
colder temperatures because of radiational cooling. This is a problem that is uniform in
mesoscale models and was expected. Temperatures over the YPG test region start out very cool
in local areas during the morning hours (just above freezing in some spots), which is a result of
light wind conditions and efficient nocturnal radiative cooling. The model was unable to capture
the observed magnitude of temperature in some of these regions (temperature biased high),
although it did capture the large local variability in the morning surface temperature field along
with the colder values in the vicinity of the meteorological surface tower sites. As an example,
table 5 displays the large variation in temperature during the morning hours on 18 December
2007. Most current-generation planetary boundary layer schemes used in NWP models such as

27

the WRF poorly handle the complex meteorological processes that occur in stable regimes. Newer schemes now in development and testing do show promise in improving stable boundary layer treatment, and may be available to the WRF in the near future (*12*). Surface temperatures did warm rapidly throughout the afternoon in the region, which again was captured well by the model although there was a slight cold bias noted.

Table 5. Sites 1 and 3 (blue font) surface weather observations during ScanEagle flight test on 18 Dec. 2007.

Time (UTC)	Wind speed (m/s)	Wind direction (deg)	T (deg C)
1500	0.4 (0.0)	160.7 (N/A)	3.3 (11.1)
1600	0.7 (1.1)	90.1 (239.5)	5.7 (10.0)
1700	0.2 (0.9)	43.8 (122.5)	10.3 (13.9)
1800	2.5 (2.4)	162.2 (114.7)	15.0 (16.2)
1900	2.5 (2.8)	150.6 (114.5)	16.7 (17.2)

New efforts will shift focus to the use of the continuous data assimilation method known as observation nudging, now a built-in feature of the WRF. This data assimilation method is more useful (versus the intermittent data assimilation method employed by LAPS) for the types of asynoptic and sporadic Army battlefield weather observations anticipated, which are comprised largely of surface sensors, tactical UAS sensors such as Tropospheric Airborne Meteorological Data Reporting (TAMDAR), and artillery radiosondes. The observation nudging will also make WRF data assimilation cycling easier to implement, and will allow for all the code (data assimilation and predictive model) to be consistent within one software package. The only true disadvantage is that observation nudging can only accept direct weather observations, whereby a variational system, like LAPS, can handle indirect weather observations such as radiances.

One considerable challenge related to 1-km grid spacing scales and hourly data assimilation cycling is there are few observation datasets available to support such high resolution and high update frequency modeling and evaluation. That is why the special YPG datasets will continue to be leveraged, even though these sets may not offer the best meteorological scenarios to demonstrate the potential impact of local, high frequency data assimilation.

The YPG studies did provide ARL an excellent opportunity to find flaws in the turbulence program that otherwise would not have been afforded since the increase in model vertical resolution provided a ground-breaking test for the software. Numerous changes in the software were made in early 2008 with an emphasis on providing a more accurate forecast for turbulence based on real-time pilot reports. In the lower levels, where the PI is used, the differential between the wind speed with height from level to level can be very small, thus the value of the RI can become excessively large. To deal with this problem, limits were set to prevent those terms from becoming too influential and dominating the total RI. When the differential between

the grid points became smaller than 0.10, the limits were adjusted to 0.10 since these small differences are not significant in the production of turbulence anyway. Another change was completed in equation 2 where the exponential in the first term, the (wind speed)^2 term, was changed to 1.8 in an effort to reduce some of the bias in turbulence forecast based just on stronger low-level wind speeds. A final modification was to adjust the categories that determine light, moderate, or severe turbulence in an effort to reduce the excessive moderate and severe turbulence forecasts.

It is uncertain how effective the changes in the low-level turbulence routines are, given the limited set of evaluated model runs. Additional testing and comparison to pilot reports will give more detailed information about improvements made in turbulence forecasting as mesoscale models trend to smaller grid sizes and additional sigma levels to provide additional detailed model forecasts. It is apparent that the routines formulated for predicting turbulence may not capture the true nature of turbulence in the atmosphere. Ongoing efforts to understand and forecast turbulence at very small scales are still being developed and will undoubtedly add insight in solving this problem. For now, the best approach is to adjust what does exist and find a fit that provides the best results and skill for the pilot and aircraft.

8. Conclusions

The WRF was run at ARL during November and December of 2007, in order to provide operational weather support for CRREL-organized ScanEagle test flights over YPG. The model results and local observations showed that the YPG region has a complex variety of low-level wind flow conditions, largely due to local variations in topography within a desert environment prone to strong daytime heating and nocturnal radiational cooling.

Additional studies need to be conducted on the forecasting of buoyancy-driven turbulence within the unstable daytime YPG boundary layer, along with nocturnal shear-driven turbulence under more stable boundary layer conditions. An important outcome of the exercises was that CAT at low levels was identified as being overforecasted by the ARL algorithm because of the impact of the very fine model resolutions on RI number computations. Subsequent improvements were made to the algorithm to reduce this effect and have been shown to produce more realistic results.

The WRF proved to be quite effective with respect to capturing local variations of the low-level winds because of topographic forcing. However, there were some identified instances where the model failed to capture these features possibly because of the lack of grid resolution or a synoptic-scale lateral boundary condition passed by NAM. Another cause of error may be land use misclassifications. Overall, the WRF proved to be capable of properly incorporating the large-scale forcing conditions passed to it from NAM and capable of reproducing much of the

local mesoscale diurnal variability because of topographical forcing during conditions of weak synoptic flow (at least that resolvable by the 1-km grid spacing). It also showed to be prone to some apparent biases, such as a slight cool bias during the peak afternoon temperature conditions and an opposite warmer bias during the pre-dawn and early morning hours. However, many more cases would need to be simulated before any definite statements about the WRF and the local YPG biases can be stated with confidence.

9. References

1. Dumais, R. E.; Passner, J. E.; Flanigan, R.; et al. High-resolution Forecasting Using the Advanced Research Version of the Weather Research and Forecast model, in support of Fall 2007 ScanEagle UAS test flight over Yuma Proving Ground, AZ., Report for U.S. Army Cold Regions Research and Engineering Laboratory, Hanover, NH, 2008.

2. Wikipedia. http://en.wikipedia.org/wiki/ScanEagle (accessed 8 January 2009).

3. National Center of Atmospheric Research. http://wrf-model.org/index.php (accessed 1 August 2008).

4. Miles, J. W.; Howard, L. N. Note on a Heterogeneous Shear Flow. *J. Fluid Mech* **2007**, *20*, 331–336.

5. Stull, R. B. *An Introduction to Boundary Layer Meteorology*; Kluwer Academic Publishers, Boston, MA, 1989, p 670.

6. Boyle, J. S. *Turbulence Indices Derived From FNOC Field and TOVS Retrievals*; NOARL Technical Note 47; Naval Oceanographic and Atmospheric Research Laboratories, 1990.

7. Ellrod, G. P.; Knapp, D. I. An Objective Clear Air Turbulence Forecasting Technique Verification and Operational Use. *Wea. Forecasting* **1992**, *7*, 150–165.

8. McCann, D. W. An Evaluation of Clear-air Turbulence Indices. Preprints of 5th International Conference on Aviation Weather Systems, Vienna, VA, 1993, Paper 8.2.

9. Passner, J. *An Evaluation of the Three-Dimensional Weather Hazards Using Sounding Data and Model Output Data*; ARL-TR-1046; U.S. Army Research Laboratory: White Sands Missile Range, NM, 2000.

10. Knapp, David I.; Smith, T. J.; Dumais, R. E. Development and Verification of a Low-Level turbulence Analysis and Forecasting Index Derived from Mesoscale Model Data, Preprint of Sixth Conference on Aviation Weather Systems, Dallas, TX, 1995, Paper 11.11.

11. Passner, J. *Using the Advanced Research Version of the Weather Research and Forecasting Model (WRF-ARW) to Forecast Turbulence at Small Scales*, ARL-TR-4575, U.S. Army Research Laboratory: White Sands Missile Range, NM 2008.

12. Sukoriansky, S; Galperin, B; Perov, V. A Quasi-Normal Scale Elimination Model of Turbulence and its Application to Stably Stratified Flows. *Nonlinear Processes in Geophysics* **2006**, *13*, 9–22.

List of Symbols, Abbreviations, and Acronyms

AFWA   Air Force Weather Agency

AGL   above ground level

ARL   U.S. Army Research Laboratory

CAT   clear air turbulence

CISD   Computational and Information Sciences Directorate

CRREL   U.S. Army Cold Regions Research and Engineering Laboratory

CVG   convergence

DEF   deformation

FNMOC   U.S. Navy Fleet Numerical Meteorological and Oceanography Center

HOTMAC   Higher Order Turbulence Model for Atmospheric Circulations

LAPS   Local Analysis and Prediction System

MSL   mean sea level

NAM   North American Mesoscale model

NCEP   National Center of Environmental Prediction

NOAA   National Oceanic and Atmopsheric Administration

PI   Panofsky Index

RI   Richardson number

RIcrit   critical Richardson number

RRTM   Rapid Radiative Transfer Model

TAMDAR   Tropospheric Airborne Meteorological Data Reporting

TI   Turbulence index

UAS   Unmanned Aerial System

UTC   universal time coordinates

VWS   vertical wind shear

WRF   Weather Research and Forecasting model

WRF-ARW   Advanced Research version of the Weather Research and Forecasting model

WRF-NMM   Non-hydrostatic Model of the Weather Research and Forecasting model

YPG   Yuma Proving Grounds

No. of Copies	Organization